Firebrands generated from a full-scale structure burning under well-controlled laboratory conditions

Sayaka Suzuki [c], Adam Brown [a,1], Samuel L. Manzello [a,*], Junichi Suzuki [b], Yoshihiko Hayashi [b]

[a] Fire Research Division, Engineering Laboratory (EL), National Institute of Standards and Technology (NIST), Gaithersburg, MD 20899-8662, USA
[b] Department of Fire Engineering, Building Research Institute (BRI), Tsukuba, Ibaraki, Japan
[c] Large Fire Laboratory, National Research Institute of Fire and Disaster (NRIFD), Chofu, Tokyo, Japan

ARTICLE INFO

ABSTRACT

Firebrand production from a real-scale structure under well-controlled laboratory conditions was investigated. The structure was fabricated using wood studs and oriented strand board (OSB). The entire structure was placed inside the Building Research Institute's (BRI) Fire Research Wind Tunnel Facility (FRWTF) in Japan to apply a wind field of 6 m/s onto the structure. As the structure burned, firebrands were collected using an array of water pans. The size and mass distributions of firebrands collected in this study were compared with sparsely available firebrand generation data from actual full-scale structure burns, individual building component tests, and historical structure fire firebrand generation studies. In this experiment, more than 90% of firebrands were less than 1 g and 56% were less than 0.1 g. It was found that size and mass of firebrands collected in this study were similar to the literature studies, yet differences existed as well. Different experimental conditions, as well as varied firebrand collection strategies, were believed to be responsible for the differences in firebrand size and mass measured in the present work, and those in the literature. The present study has provided much needed data on firebrand generation from structures.

Published by Elsevier Ltd.

1. Introduction

Firebrands are a critical mechanism of fire spread in large outdoor fires, such as urban fires in Japan and wildland–urban interface (WUI) fires common in Australia, Southern Europe, and the USA. While firebrands have been studied for some time [1], most of these studies have focused on spotting distance [2–12]. Unfortunately, very few studies have been performed regarding firebrand generation [13–15] and the subsequent ignition of building materials or vegetative fuels by firebrands [16–19]. To develop scientifically based mitigation strategies for urban/WUI fires, such as hardening structures to make them more ignition resistant, it is necessary to understand the firebrand generation process from structures.

Sparse data exist with regard to fire size distributions from actual structures or WUI fires [20–23]. It is believed that in WUI fires, the structures themselves may be a large source of firebrands, in addition to the vegetation. Yet, due to lack of quantitative information available on production of firebrands from structures, it cannot be determined if firebrand production from

structures is a significant source of firebrands in WUI fires. Detailed studies are needed to address this question.

For completeness, prior firebrand generation studies from structures are reviewed. Vodvarka [20] measured firebrand deposition by laying out 3 m × 3 m sheets of polyurethane plastic downwind from five separate residential buildings burned in full-scale fire experiments. Three of the structures were standard frame construction with wood siding. The fourth was asphalt siding applied over sheet rock which covered the original shiplap. The fifth structure was a brick veneer over a wood frame. The total number of firebrands collected from these structure fires was 4748. Very small firebrands dominated the size distribution with 89% of the firebrands less than 0.23 cm^2.

Vodvarka [21] measured the fire spread rate radiant heat flux, firebrand fallout, buoyancy pressures, and gas composition from eight separate buildings. Firebrands were collected by laying out sheets of polyurethane plastic downwind from three of eight experiments. Two of the buildings were all wood construction, one was cement-block construction, and had wooden floors and asphalt shingles over wood sheathing. In total, 2357 firebrands were collected. More than 90% of the firebrands had a projected area less than 0.90 cm^2 and 85% of the firebrands were less than 0.23 cm^2 in projected area. Only 14 firebrands had projected areas larger than 14.44 cm^2 in three experiments.

Yoshioka et al. [24] measured the size and mass of firebrands from the real-scale wooden house in the Building Research Institute's (BRI) Fire Research Wind Tunnel Facility (FRWTF) in Japan. This is the only full-scale structure experiment under laboratory conditions with a controlled applied wind field the authors are aware of in the literature. The FRWTF is a remarkable wind tunnel because it was designed specifically with fire testing in mind. Two square pans, both 1 m × 1 m, were placed 2 m from the house to collect firebrands: one was filled with water (wet pan) and the other without water (dry pan). The total number of firebrands collected in their study was 430; 368 from a wet pan and 62 from a dry pan. It was reported that 83% of the firebrands in the wet pan were between 0.25 cm^2 and 1 cm^2 projected area while 53% of those from the dry pan were between 0.25 cm^2 and 1 cm^2 projected area. Only 1 of 368 in the wet pan and 4 of 62 in the dry pan were larger than 4 cm^2 projected area. It was pointed out that the reason why a dry pan had far less firebrands with projected areas between 0.25 cm^2 and 1 cm^2 was that they simply burned in the dry pan. The work is very important; nevertheless since construction practices in Japan are very much different than those in the USA, it is not clear how applicable this data is in terms of the WUI fire problem in the USA.

Suzuki et al. [25] collected firebrands from a two story house located in Dixon, CA. Debris piles were used to ignite the structure and it took approximately two hours after ignition for complete burn down. A large amount of water was poured onto the structure several times to control the fire since the house was located in a populated section of downtown Dixon. Firebrands were collected with a series of water pans placed near (4 m) the structure and on the road about 18 m downwind of the structure. For the data collected from the full-scale structure burn by Suzuki et al. [25], 139 firebrands were collected at the two measurement locations. All the firebrands collected from the burning house were less than 1 g and almost 85% of the firebrands collected 18 m from the structure, and 68% of firebrands 4 m from the structure, were less than 0.1 g. In terms of the projected area, most of the firebrands, 95% of those from 18 m downwind from the structure, and 96% of those 4 m from the structure, were less than 10 cm^2 in projected area.

Most recently, Suzuki et al. [26] investigated firebrand production from real-scale building *components* under well-controlled laboratory conditions using BRI's FRWTF in Japan. Specifically, wall and re-entrant corner assemblies were ignited and during the combustion process, firebrands were collected to determine the size/mass distribution generated from such real-scale building components under varying wind speed. The purpose of those experiments was to determine if useful information regarding firebrand generation may be obtained from simple components tests. Components experiments are far simpler than full scale structure experiments. It was observed that similar mass classes of firebrands were observed from components to the available full scale structure tests in the literature. The results of Suzuki et al. [26] are compared to the experiments outlined in this paper and are presented below.

Finally, it is worth mentioning that Manzello and Foote [23] examined the size distribution of firebrand exposure during the Angora fire, a severe WUI fire in California, USA in 2007. In that study, a trampoline, which was exposed to wind-driven firebrands during the fire, was collected for analysis. The burn areas of the round trampoline base were assumed to be generated from firebrands and measured by digital image analysis. The trampoline section that was analyzed had an overall area of 10.5 m^2 with 1800 burn holes. The single largest hole in the trampoline base had a 10.25 cm^2 burned area. It was observed that more than 85% of the burned areas from firebrands were less than 0.5 cm^2 and more than 95% of them were less than 1.0 cm^2. In addition to the trampoline data, burn patterns on building materials and plastic outdoor furniture were observed at 212 individual locations on or near numerous buildings in the Angora Fire. A large majority of these firebrand indicators were less than 0.40 cm² with the largest being 2.02 cm² or 0.64 cm × 3.18 cm. Most of the burn patterns on building materials consisted of shallow scorch or char marks on wooden or composite lumber decks.

To this end, firebrand production from real-scale building under well-controlled laboratory conditions was investigated. The structure was fabricated using wood studs and oriented strand board (OSB). A sofa was placed inside the structure and this sofa was ignited using a remotely controlled electric match (matchbook coupled to resistive wire; electrical current provide by battery box). The door opening was sized to allow flashover to occur inside the structure. The entire structure was placed inside the BRI's FRWTF in Japan in order to apply a wind field of 6 m/s onto the structure. As the structure burned, firebrands were collected using an array of water pans positioned downstream of the structure. The size and mass distributions of firebrands collected were compared with firebrand generation data from actual full-scale structure burns, individual building component tests, and historical firebrand generation studies from structures. This study provides data for the beginning of a database on firebrand generation data from structures that is being developed by Manzello and co-workers. Temperatures and mass loss measured during the experiment are also reported in this paper.

2. Experimental description

A full-scale structure was constructed for the experiments. The overall dimensions of the structure were 4 m long by 3 m wide by 4 m high. Fig. 1 displays an image of the structure. The wall framing was constructed of wood studs (wood cross section 3.8 cm by 8.8 cm) spaced 406 mm on center (16.0″). King post trusses were used for the roof assembly with a roof pitch of 20° as these are thought to be one of the simplest trusses for roof assemblies with overhang used in the USA. The supporting structure for the roof assembly was constructed with wood studs (wood cross section 3.8 cm by 14.0 cm). Oriented strand board (OSB) with a thickness of 11 mm was applied to the exterior walls and roof. The moisture content of the building materials was nominally 10% (dry basis). A schematic drawing is shown in Fig. 1. The entire structure was placed on load cells to determine the temporal variation of mass loss. The total mass of the structure at
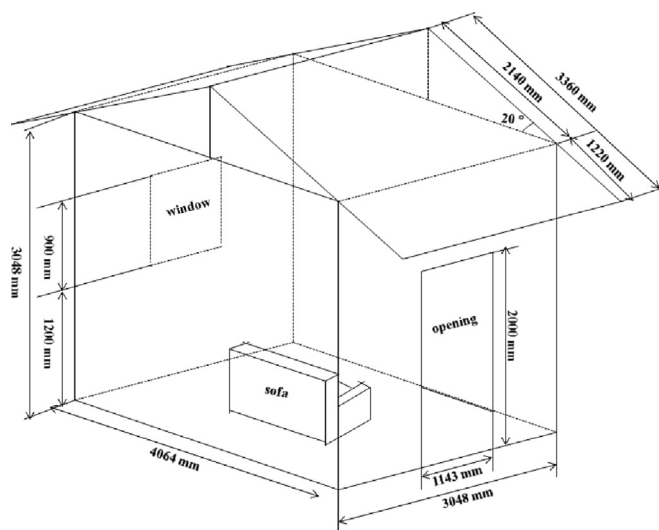

Fig. 1. Schematic of the structure.

ignition was 1973 kg $\pm$ 4.0 g. Great care was taken to protect the load cells from the thermal insult of the fire (described later). Temperature measurements were made at all four load cell locations to verify that the load cells did not heat up appreciably during the experiments. In addition, temperature measurements using bare bead thermocouples were made inside the structure to provide information on the gas-phase temperatures produced during the combustion process. The measurements were made 1.0 m from the ceiling and 1.0 m from floor. It is well known that bare bead thermocouple measurements in fire environments are prone to errors due to radiative heat transfer [27]. While aspirated thermocouples can reduce such errors, it does not eliminate them. Accordingly, it was decided to not add the complexity of aspirated thermocouples for the gas phase measurements in these experiments. The gas phase measurements are not corrected for radiative effects, since such corrections require properties that were not quantified in the fire environment (e.g. thermocouple bead emissivity, local gas velocity/composition, local radiation environment) [27]. Therefore, the standard uncertainty (based on expert judgement) in these measurements was estimated to be 25% [27]. The structure was intentionally left unfinished on the inside. No siding treatments were installed on the façade of the structure since the purpose was to demonstrate the feasibility of this type of experiment.

The structure was installed inside the test section of the FRWTF at BRI shown in Fig. 2. The facility was equipped with a 4.0 m diameter fan to produce a wind field up to a 10 m/s. The uniformity of the wind velocity distribution was verified using a 21 point hot wire anemometer array. The flow was uniform
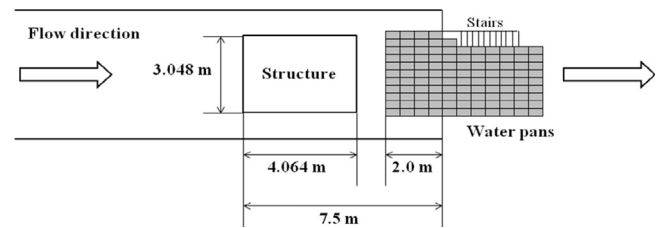
a

b

Fig. 2. Pictures of the structure at the onset of the experiment. (a) From inside wind tunnel, (b) from outside wind tunnel.

Fig. 3. Location inside the FRWTF.

(to within 10%) across the entire length of the 15 m test section. To track the evolution of the size and mass distribution of firebrands, a series of water pans was placed downstream of the assemblies. The wind tunnel speed was fixed at 6 m/s and was maintained throughout the experiment; it was switched on just prior to ignition of the sofa (described below). This speed was selected to be able to compare results to literature studies [25,26].

A very important aspect of this study was to determine the best ignition method in order to provide conditions to collect firebrands during the combustion of the structure. It is important to realize that it is very difficult to simulate the conditions of an actual WUI fire in a controlled laboratory setting. A sofa was used to generate flashover inside the structure. This sofa was ignited using a remotely controlled electric match (matchbook coupled to resistive wire; electrical current provide by battery box) and the door opening was sized to allow flashover to occur inside the structure in order to produce ignition. This ignition scenario was tied to a real WUI fire by assuming firebrands would be able to penetrate the structure envelope and produce ignition inside the structure. Extensive work by Manzello et al. [28–35], using the NIST Dragon, has demonstrated that structures are vulnerable to wind-driven firebrand showers so this type of ignition scenario is not unrealistic. Future experiments are planned to ignite structures from the outside (such as the type of ignition that would expected from firebrand attack that ignited fine fuels adjacent to structures or direct flame contact from nearby fuels such as shrubs or trees) to determine if the ignition method has any bearing on the firebrand generation process.

Firebrands were collected by using a series of water pans placed behind the structure shown in Fig. 3. Water was necessary to quench the burning firebrands. After deposition into the water pans, firebrands were filtered from the water using a series of fine mesh screens. Firebrands were then dried in an oven at 104 °C for 24 h. The mass and size of each firebrand was measured by a precision balance (0.001 g resolution) and using digital image analysis (described in detail below), respectively.

3. Results and discussions

Fig. 4 displays images of the structure as the combustion process unfolded. As mentioned above, the wind tunnel speed was fixed at 6 m/s and was kept on prior to igniting the sofa using the electrical match system. It was very interesting to observe the firebrand generation process. Over the course of the experiment, firebrands were produced as the oriented strand board (OSB) began to weaken and break up due to the continued combustion process. As the experiment progressed, eventually all the OSB was consumed but the wood studs remained.

The experiment continued for almost 11 min 30 s before water was applied for extinguishment in order to prevent the entire structure framing from collapsing, and prevent destruction of the collection pans. Complete structure collapse would also be expected to contribute to the firebrand generation process but was not possible for the purposes of the present experiments since
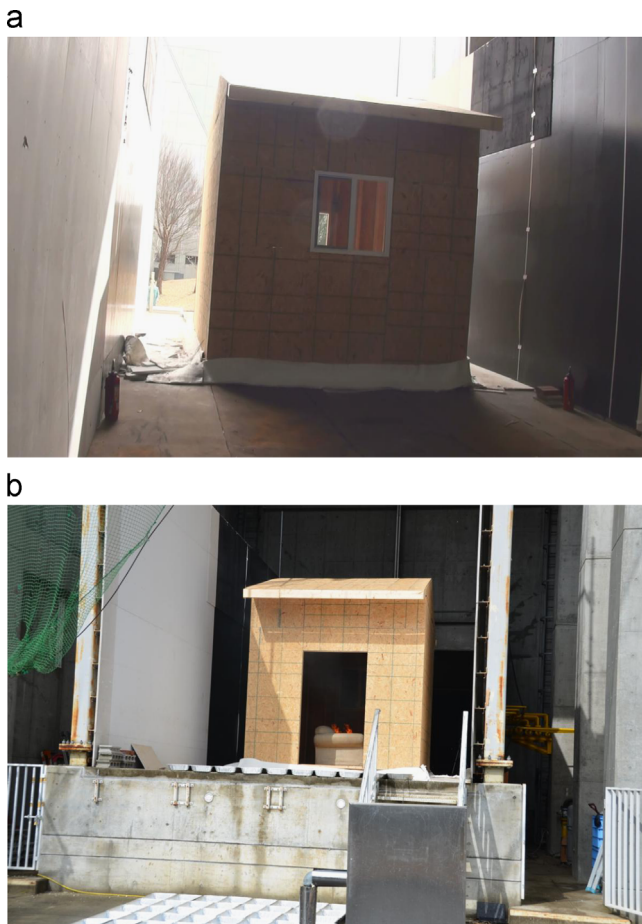
Fig. 4. Images of the structure as the combustion process unfolded. (a) 4 min 30 s after ignition, (b) 9 min after ignition, (c) 10 min after ignition, (d) 11 min after ignition.
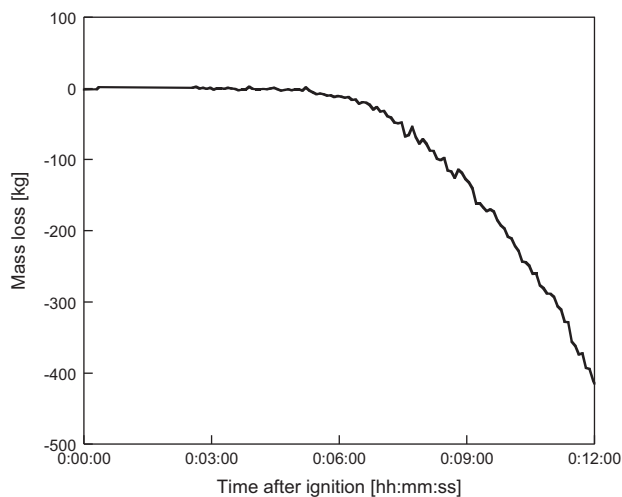

Fig. 5. Temporal profile of mass loss.

Fig. 6. Temporal profile of mass loss rate per unit area.

it would disrupt the firebrand collection pans. Time zero was set to the time when the sofa was ignited by the electric match. Smoking inside the structure was first observed at 1 min 30 s and flames on the sofa were visually observed at around 3 min. The left and right hand sides of the window broke 4 min 45 s and 4 min 20 s, respectively. The flames started growing over the roof at 5 min 45 s, and then it was observed the OSB began to weaken and break up at 7 min 20 s. OSB continued to weaken and at the end of the experiment, at 11 min 30 s, wood studs were left with almost no OSB.

Fig. 5 displays the temporal evolution of mass loss. The uncertainty in the mass los measurement is provided below. It would be expected that the wind load on the structure may provide an artificial load on the structure and affect the mass loss
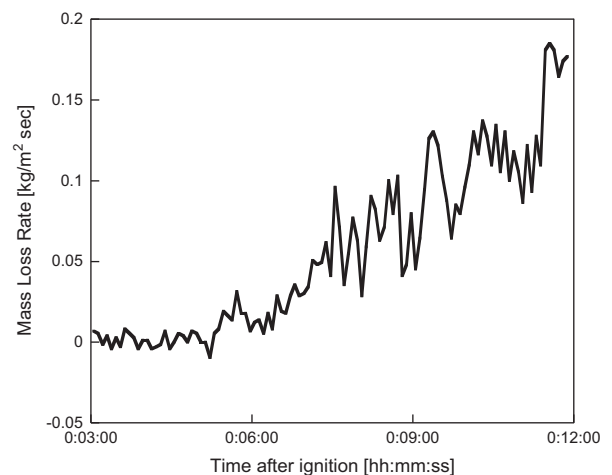
measurement. To reduce this affect, the wind tunnel was turned on prior to the actual experiment with the structure in place to determine the degree of offset produced. This offset was then subtracted from the mass loss measurement. Minimal mass loss was observed during the first 5 min, the initial stage of combustion, and then the structure lost its mass gradually over the next 7 min. In the early stages of the experiment, prior to flashover, only the sofa was engaged in the combustion process. The mass of the sofa was 98 kg, which corresponded to 4.5% of total mass. The burned structure was not completely consumed, which is why the total mass loss was far less than the initial mass.

The temporal variation of the mass loss rate per unit area, between 3 min and 12 min, during burning, is shown in Fig. 6. The temporal variation of mass loss rate per unit area was calculated based on the floor area of the structure, 12 m². The mass loss rate

per unit area was nearly zero until 6 min, and then started slowly increasing. It was observed that mass loss rate per unit area stabilized around 0.1 [kg/m² s] (between 9 min to 12 min). The mass loss rate per unit area dramatically increased at the very end of the experiment. Yoshioka et al. [24] calculated the mass loss rate per unit area of their experiment performed at the FRWTF and reported a value of 0.05 [kg/m² s] under 4 m/s wind speed, which is almost half the value of the experimental results described in this paper. They also performed experiments under 3 m/s and 6 m/s imposed wind, and showed that the mass loss rates per unit area were 0.06 [kg/m² s] for both wind speeds [36]. It is known that ventilation is an important aspect in compartment fire dynamics [37]. While the structure in this experiment had a 2000 mm × 1143 mm opening on the downwind side and a 900 mm × 900 mm opening on the upwind side, the structure in Yoshioka's studies [24,36] had 1820 mm × 846 mm openings on both sides. The overall size of structure in this experiment and Yoshioka's experiments were comparable, and the conditions for ventilation were similar as well. Therefore, different ventilation conditions are not believed to be the dominant reason for different mass loss rates per unit area observed in these experiments. Rather, the structures used in their experiments were wooden structures with Japanese slate roofing and outer wall siding (mortar). The burning behavior of their structures was affected by roofing and siding materials since slate and mortar are not combustible. The structure used in this experiment was constructed entirely of OSB/wood studs, and was not finished on the interior, so it would be expected that the mass loss rate per unit area would be larger.

As mentioned before, the load cells used for mass loss measurement were protected. The load cells employed in this work had an operating temperature range between −30 °C to +80 °C. Above this temperature range, the load cells may be damaged and result in error. A picture and the schematic of the custom thermal protection system designed for the load cells are shown in Fig. 7(a) and (b), respectively. The load cells were placed in small fitted boxes made from calcium silicate boards, then covered with ceramic fiber blanket. Metal plates were placed between gypsum board and the structure to improve the precision of the load cell measurements. Thermocouples were attached to the top of the load cells in order to measure the temperature rise of the load cells
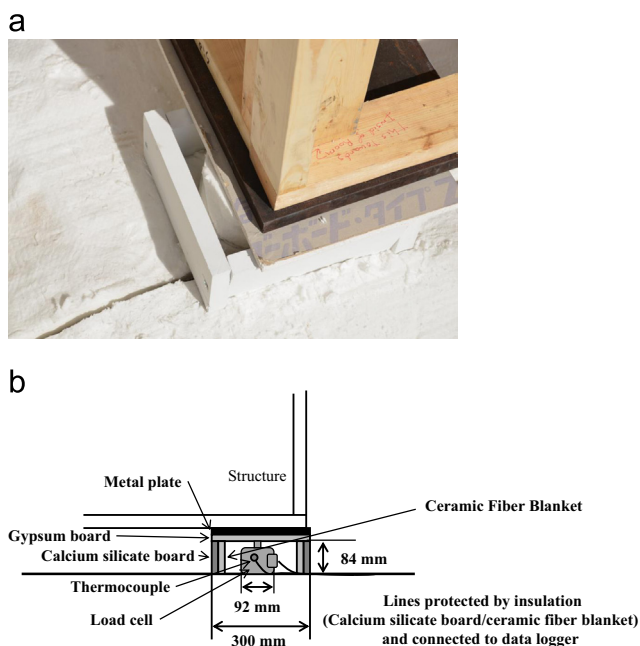
during the fire experiment. The thermocouples used in this study were type K thermocouples. Fig. 8 shows the temperature profiles of each load cell used. The maximum temperature during all these measurements was 31.4 °C; well within the operating range. This shows that the load cell protection method used in this experiment was effective to shield them from heat generated by the intense combustion of the structure. Accordingly, the standard uncertainty in the mass loss measurements was ± 1% (based on manufacturer specifications with correction applied for the measured temperature increase).

Measurements were also made inside the structure to provide information on the gas-phase temperatures produced during the combustion process. The measurements were made 1.0 m from the ceiling and 1.0 m from floor shown in Fig. 9. Bare bead thermocouples were used and these were the same type as those attached to the load cells described in the previous section. The uncertainty in the gas phase temperature measurements using bare bead thermocouples are described earlier. Both temperature profiles were observed to be similar. The temperature rapidly increased at about 5 min due to the increased oxygen supply due to the breaking window which occurred around 4 min 45 s and 4 min 20 s at the left and the right hand sides of the window. The temperature at both heights peaked at about 780 °C at 9 min 53 s, and 9 min 28 s, respectively, for the measurements at 1.0 m

Fig. 7. Images of load cell protection. (a) Picture of load cell protection, (b) schematic of load cell protection.
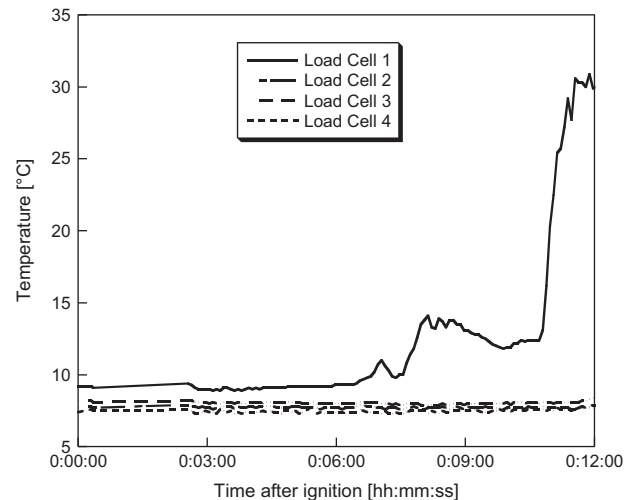

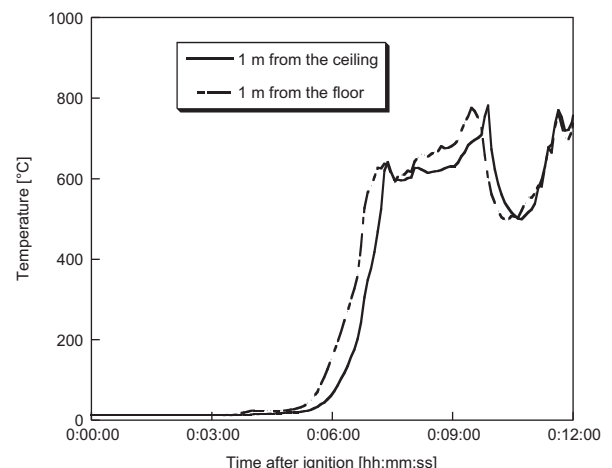**Fig. 8.** Temperature profile measured at load cells.

Fig. 9. Temperature profile measured inside the structure.

from the ceiling and 1.0 m from the floor. After the peak, the temperatures diminished to about 500 °C.

Fig. 10 shows the size and mass distribution of firebrands collected from the burning structure in this study. The total number of firebrands collected using the pan array was 473 and all the data is shown in Fig. 10. Image analysis software was used to determine the projected area of a firebrand by converting the pixel area using an appropriate scale factor [25]. It was assumed that deposited firebrands would rest flat on the ground and the projected areas with the maximum dimension and the second maximum dimension of three dimensions were measured (for cylindrical or flat shaped firebrands, respectively) [25]. Images of well-defined shapes (e.g. circular objects) were used to determine the ability of the image analysis method to calculate the projected area [25]. Based on repeat measurements of different areas, the standard uncertainty in determining the projected area was $\pm\,10\%$. Repeat measurements of known calibration masses were measured using the balance used for the firebrand mass analysis. The standard uncertainty in the firebrand mass was $\pm\,1\%$. The largest firebrand collected had a projected area of 45 cm^2
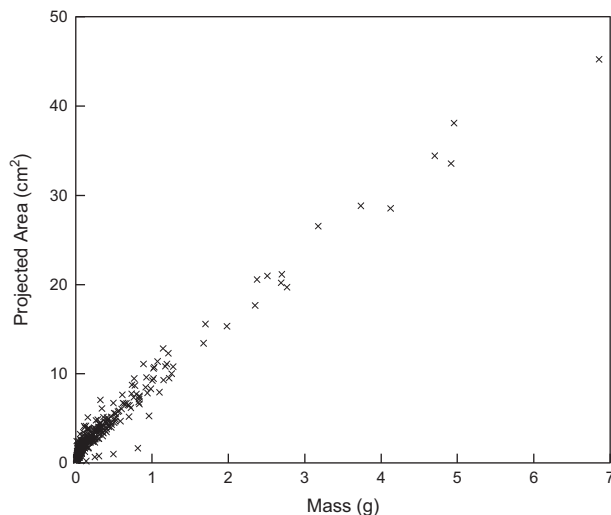

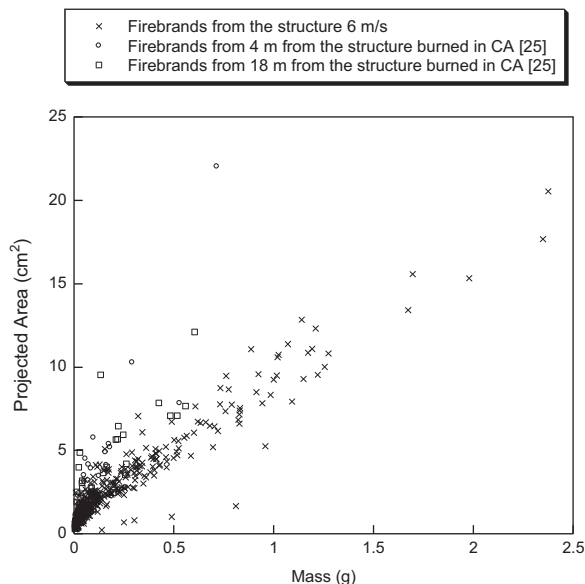**Fig. 10.** Size and mass distribution of firebrands collected in this study.

with mass of 6.8 g. More than 90% of the total number of firebrands collected in the pans had less than 1 g mass and 56% had less than 0.1 g mass. In terms of the projected area, more than 90% of the firebrands were less than 10 cm^2 with 25% less than 1 cm^2.

In Fig. 11, the size and mass distribution of firebrands collected in this study are compared with those obtained from an actual full-scale structure burn conducted in Dixon, CA [25]. In order to show a detailed comparison, the range in the size and the mass was limited to between 0 cm^2 and 25 cm^2, and between 0 g and 2.5 g, respectively, since the majority of firebrands collected were within this range. The firebrands in this study were observed to be larger than the firebrands collected from an actual full-scale house burn in CA [25]. In addition, it was found that some of firebrands collected from the full-scale structure burn in Dixon, CA were lighter in mass for the same projected areas than those collected from this experiment. Yet, most of firebrands were found to be within the same range. While it was possible to control the wind speed in the Dixon, CA experiment, as it was a burn down of an existing structure, the prevailing wind was 6 m/s during the test, similar to the wind tunnel speed in this experiment. In the full-scale house burn experiment, a large amount of water was poured onto the structure several times to control the fire since the house was located in a populated section of downtown Dixon. Other differences are related to the construction materials. Materials used for the structure burned in this study were OSB/wood studs with no siding applied while the structure that was burned in Dixon, CA was fitted with wood siding, tar paper, and plywood. It is thought that this variety of materials in the structure may be responsible for lighter firebrands.

The size and mass distribution of firebrands in this study were also compared with those from individual building components tests [26] (Fig. 12). Again, to be able to show the detailed comparison, the range of the size and the mass is limited to between 0 cm^2 and 25 cm^2, and up to 2.5 g, respectively. The materials used were the same in all of experiments (OSB/wood studs). For detailed comparison, it is appropriate to compare firebrands collected under similar conditions. Namely, two of the
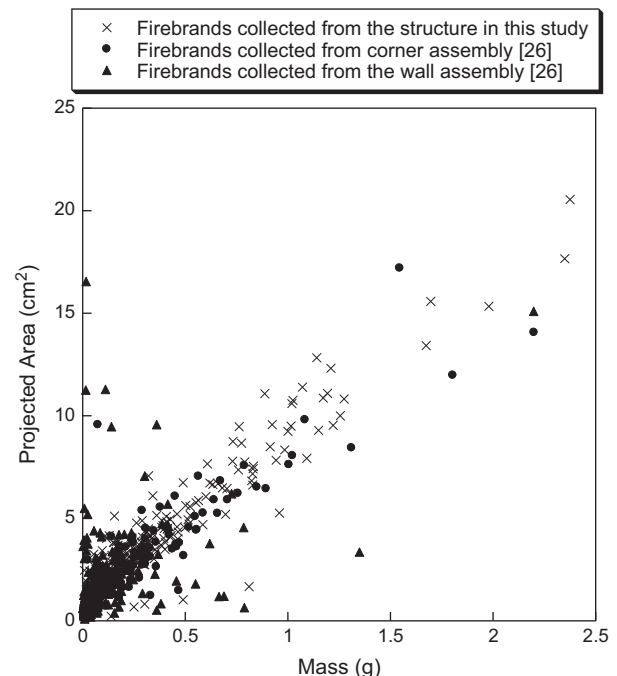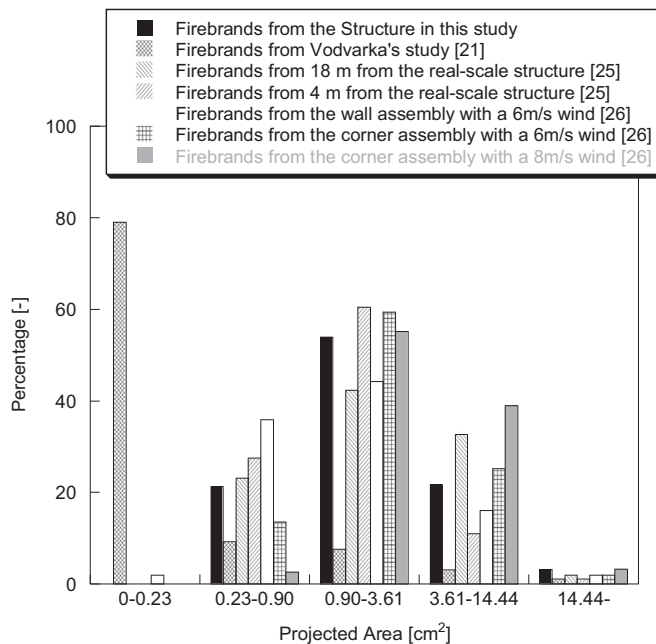

Fig. 11. Comparison of size and mass distribution with full-scale structure burn in Dixon, CA [25].

Fig. 12. Comparison of size and mass distribution with components test under the similar laboratory condition [26].

Table 1
Detailed information on compared experiments.

	Peak fire intensity	Material used	Wind speed	Mesurement techniques	Significant results
Full-scale burn in this study	1.76 MW/m^2	OSB and 2 × 4	6 m/s	Pans filled with water	More than 90% of firebrands were less than 1 g More than 90% of the firebrands less than 10 cm^2
Vodvarka [20]	Not provided	Standard frame construction with wood siding/asphalt siding applied over sheet rock/brick veneer over a wood frame	Not specified	Sheets of polyurethane plastic	89% of firebrands less than 0.23 cm^2
Vodvarka [21]	Not provided	All wood construction/cement-block construction with wooden floors and asphalt shingles over wood sheathing	Not specified	Sheets of polyurethane plastic	85% of firebrands less than 0.23 cm^2
Yoshioka et al. [24,36]	1.08 MW/m^2	Fire prevented wood with outer wall siding and slate roofing	4 m/s	Pan filled with water and no water	83% of firebrands in the wet pan between 0.25 and 1 cm^2
Full-Scale Burn in CA [25]	Not measured	Wood and blick	6 m/s	Pans filled with water	All the firebrands less than 1 g Most of the firebrands less than 10 cm^2
Components [26]	Not measured	OSB and 2 × 4	6 m/s 8 m/s	Pans filled with water	More than 90% of firebrands were less than 1 g More than 90% of the firebrands less than 10 cm^2

*Peak fire intensity was estimated based on mass loss rate per unit area and the heat of combustion of wood.

Fig. 13. Comparison of size distributions with Vodvarka [21].

Legend:
- Firebrands from the Structure in this study
- Firebrands from Vodvarka's study [21]
- Firebrands from 18 m from the real-scale structure [25]
- Firebrands from 4 m from the real-scale structure [25]
- Firebrands from the wall assembly with a 6m/s wind [26]
- Firebrands from the corner assembly with a 6m/s wind [26]
- Firebrands from the corner assembly with a 8m/s wind [26]

experiments in our previous study (Experiment No. 1 and No. 2) were performed under 6 m/s condition, which are the same wind speed as in this experiment. Experiment No. 1 was performed with the wall assembly and Experiment No. 2 was performed with the re-entrant corner assembly, both were ignited with t-shaped burner from the upwind side. It was reported that 65% and 37% of the firebrands from Experiment No. 1 and No. 2 were less than 0.1 g and that 98% and 94% of them were less than 1 g, respectively. In this experiment, more than 90% of firebrands were less than 1 g and 56% of them were less than 0.1 g. It shows that firebrand from both Experiment No. 1 and No. 2, and this experiment was quite similar in their mass range. Obviously the structure contained both corners and walls and it shows that

firebrands collected from the structure had similarity to firebrands that were generated from both individual corner assemblies and wall assemblies.

Firebrands collected in this study were also compared with data from the literature [20,21,24]. Detailed information for each burn is provided in Table 1, including experiments from individual component tests [26]. Fire intensity was estimated based on mass loss rate per unit area and the heat of combustion. The heat of combustion for wood, 17.76 kJ/g, was used for the estimation [38]. Fig. 13 shows the comparison with data from Vodvarka [21] along with previous other data [25,26]. It is important to compare current experimental data with any previous available literature data, since such sparse data exists. It is also important to compare current data with previous data in order to see if the firebrands collected under laboratory (controlled) conditions may provide any insight into firebrand generation from a full scale house burn under ambient conditions. In Vodvarka's study, around 80% of firebrands had less than 0.23 cm^2 projected area while in our experiment, none of firebrands were found to have less than 0.23 cm^2. In the contrast, most of firebrands collected in this study were between 0.90 cm^2 and 3.61 cm^2, which is similar to the ones collected in previous studies [25,26]. The difference between Vodvarka's study [21] and this study is the method to collect firebrands. A series of water pans was used to collect firebrands in this study while the polyurethane sheets were used and the burned area was measured in Vodvarka's study. Differences in these collection methods may be the reason for the observed differences in collected firebrand sizes.

Firebrand data from Yoshioka et al. [24] was also compared with data from this experiment as well as previous studies [25,26] (Fig. 14). In Yoshioka et al. [24], two different pans were used to collect firebrands: one was filled with water (wet pan) and the other was with no water (dry pan). It is not clear why a dry was used since it is not able to quench combustion of the generated firebrands. Eighty three percent of firebrands collected in the wet pan were between 0.25 cm^2 and 1 cm^2 projected area while only 21% of firebrands in this study were in that range. Only 1 of 368 firebrands collected in the wet pan were more than 4 cm^2 in projected area. On the contrary, about 20% of firebrands collected
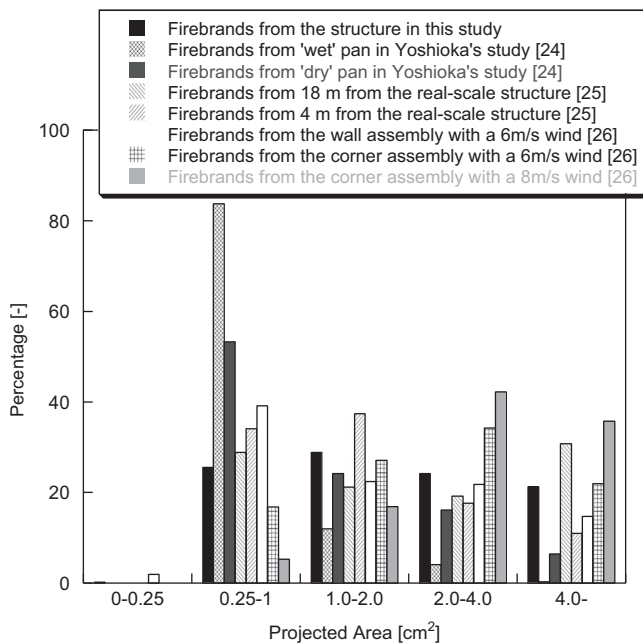
Fig. 14. Comparison of size distributions with Yoshioka et al. [24].

in this experiment were larger than $4\,cm^2$. The differences between Yoshioka et al. [24] and this study were the wind speed, the construction materials, the location, and collection area of the pans as shown in Table 1. In this study, a series of water pans were located downwind from the structure to collect firebrands; thus the area for firebrand collection in this study was much larger than the one in Yoshioka et al. [24]. This is probably the reason why a broader size and mass class of firebrands were collected in this study, compared to Yoshioka et al. [24].

4. Summary

Firebrand production from real-scale building under well-controlled laboratory conditions was investigated. The structure was fabricated using wood studs and OSB. A sofa was placed inside the structure and this sofa was ignited using a remote electric match. The door opening was sized to allow flashover to occur inside the structure in order to produce ignition. The entire structure was placed inside the BRI's FRWTF in order to apply a uniform wind field of 6 m/s onto the structure. As the structure burned, temperatures inside the structure were measured by thermocouples and the mass loss of the structure was measured by load cells. Firebrands were collected using an array of water pans.

The mass and size of firebrands collected in this study were compared with those from previous studies [21,24–26]. It was observed that the mass and size of the majority of firebrands collected in this study were less than 1 g and less than $10\,cm^2$, which is similar to previous experiments [21,24–26]. Comparison with the firebrands from Vodvarka [21] showed that the firebrands from this study were larger and broader in size distribution. These differences are believed to be due to different firebrand collection methods. Comparison with the firebrands from a full-scale burn in CA [25] showed that the firebrands from this study were slightly heavier in mass, at a given projected area. Materials used for the structure burned in this study were OSB/wood studs with no siding applied while the structure that was burned in Dixon, CA [25] was fitted with wood siding, tar paper, and plywood. It is thought that this variety of materials in the structure may be responsible for lighter firebrands. The firebrands from this study

were found to be larger and the size distribution of the firebrands from this study was found to be broader than those from Yoshioka's study [24] due to the larger area firebrand collection location.

This experiment produced similar firebrands, in mass ranges to the experiments performed under similar conditions with the wall and the re-entrant corner assemblies [26]. These comparisons showed that the experiment performed in this study, under controlled conditions with simplified construction methods, could provide useful information on firebrand production measured in far more complex situations, such as real-scale structure burns [25].

The research described here has been focused on fundamental aspects of firebrand production from a full-scale structure under an applied wind field. This work is a natural extension of prior work by Suzuki et al. [26] to determine firebrand production following fire testing of individual components under laboratory conditions. While structures in WUI communities are made from various materials, the structure used for this experiment were simplified (OSB and wood studs only—common base materials for USA construction), in order to demonstrate the feasibility of such testing and attempt to determine rate limiting materials for firebrand production. It is important to perform more experiments which will more closely replicate real construction under well-controlled conditions. Specifically, adding siding or roofing materials should be the next step. Additional wind speeds and time varying wind fields would be highly desirable to experiment with as well.

The type of data collected as part of this effort is required to advance the modeling of fire behavior in WUI environments. Firebrands are a major ignition source in WUI fires and several models have been trying to capture firebrand behavior in order to evaluate the likelihood of structure ignition caused by firebrands [10,39]. However, lack of fundamental data of firebrand generation has made it difficult to advance these models. Adding the firebrand data collected from this study will enable further advances for these models. As an example, the Wildland Fire Dynamic Simulator (WFDS) remains in the validation stages [40]. It is thought that this data will be added to previous data set and eventually be used to incorporate source terms for firebrand generation from structures into WFDS.

Finally, the size and mass of firebrands generated by the NIST Dragon have been tied to those measured from vegetation [14,16] and a real WUI fire (Angora) [23]. Firebrands in WUI fires are thought to be produced from structures, not only vegetation, and this work is providing detailed understand of this production process for the first time. The size and mass distribution collected in this study will be of use to allow the Dragon to produce firebrand showers typical of burning structures.

References

[1] E. Koo, P.J. Pagni, D.R. Weise, J.P. Woycheese, Int. J. Wildland Fire 19 (2010) 818–843.
[2] F. Albini, Spot Fire Distances From Burning Trees—A Predictive Model, USDA Forest Service General Technical Report INT-56, Missoula, MT, 1979.
[3] F. Albini, Transport of firebrands by line thermals, Combust. Sci. Technol. 32 (1983) 277–288.
[4] A. Muraszew, J.F. Fedele, Statistical Model for Spot Fire Spread, The Aerospace Corporation Report No. ATR-77758801, Los Angeles, CA, 1976.
[5] C.S. Tarifa, P.P. del Notario, F.G. Moreno, Proc. Combust. Inst. 10 (1965) 1021–1037.
[6] C.S. Tarifa, P.P. del Notario, F.G. Moreno, Transport and Combustion of Fire Brands. Instituto Nacional de Tecnica Aeroespacial "Esteban Terradas", Final Report of Grants FG-SP 114 and FG-SP-146, Vol. 2. (Madrid, Spain) 1967.
[7] S.D. Tse, A.C. Fernandez-Pello, Fire Saf. J. 30 (1998) 333–356.
[8] R. Anthenian, S.D. Tse, A.C. Fernandez-Pello, Fire Saf. J. 41 (2006) 349–363.
[9] J.P. Woycheese, Brand Lofting and Propagation for Large-scale Fires, Ph.D. Thesis, University of California, Berkeley, USA, 2000.
[10] K. Himoto, T. Tanaka, Fire Saf. Sci. 8 (2005) 433–444.
[11] I.K. Knight, Fire Technol. 37 (2001) 87–100.

[12] H.H. Wang, Fire Technol. 47 (2011) 321–340.
[13] T.E. Waterman, Experimental Study of Firebrand Generation, IIT Research Institute, Project J6130, Chicago, IL, 1969.
[14] S.L. Manzello, A. Maranghides, W.E. Mell, Int. J. Wildland Fire 16 (2007) 458–462.
[15] S.L. Manzello, A. Maranghides, W.E. Mell, Y. Hayashi, D. Nii, Fire Mater. 33 (2009) 21–31.
[16] T.E. Waterman, A.E. Takata, Laboratory Study of Ignition of Host Materials by Firebrands, Project J-6142 OCD Work Unit 2539A, IIT Research Institute, Chicago, IL, 1969.
[17] V.P. Dowling, Fire Saf. J. 22 (1994) 145–168.
[18] P.F. Ellis, The Aerodynamic and Combustion Characteristics of Eucalypt Bank—A Firebrand Study, Ph.D. Dissertation, Australian National University, Australia, 2000.
[19] A. Ganteaume, C. Lampin-Maillet, M. Guijarro, C. Hernando, M. Jappiot, T. Fonturbel, P. Perez-Gorostiaga, J.A. Vega, Int. J. Wildland Fire 18 (8) (2009) 951–969.
[20] F.J. Vodvarka, Firebrand Field Studies—Final Report, IIT Research Institute, Chicago, IL, 1969.
[21] F.J. Vodvarka, Urban Burns-Full-scale Field Studies—Final Report, IIT Research Institute, Chicago, IL, 1970.
[22] V. Babrauskas, Ignition Handbook, Fire Science Publishers, Issaquah, WA, 2003.
[23] S.L. Manzello, E.I.D. Foote, Fire Technol., published on-line (2013). http://dx.doi.org/10.1007/s10694-012-02954.
[24] H. Yoshioka, Y. Hayashi, H. Masuda, T. Noguchi, Fire Sci. Technol. 23 (2004) 142–150.
[25] S. Suzuki, S.L. Manzello, M. Lage, G. Laing, Int. J. Wildland Fire 21 (2012) 961–968.
[26] S. Suzuki, S.L. Manzello, Y. Hayashi, Proc. Combust. Inst. 34 (2013) 2479–2485.
[27] W. Pitts et al., in: Proceedings of the First Joint Meeting of the U.S. Sections of the Combustion Institute, March, 1999.
[28] S.L. Manzello, J.R. Shields, J.C. Yang, Y. Hayashi, D. Nii, in: Proceedings of the 11th International Conference on Fire Science and Engineering (INTERLFAM), Interscience Communications, London, 2007, pp. 861–872.
[29] S.L. Manzello, J.R. Shields, Y. Hayashi, D. Nii, Fire Saf. Sci. 8 (2009) 143–154.
[30] S.L. Manzello, Y. Hayashi, Y. Yoneki, Y. Yamamoto, Fire Saf. J. 45 (2010) 35–43.
[31] S.L. Manzello, S.H. Park, J.R. Shields, S. Suzuki, Y. Hayashi, Fire Saf. J. 46 (2011) 568–578.
[32] S.L. Manzello, S. Suzuki, Y. Hayashi, Fire Saf. J. 50 (2012) 25–34.
[33] S.L. Manzello, S. Suzuki, Y. Hayashi, (2011) in: Proceedings of JAFSE (Japan Association for Fire Science and Engineering) Annual Symposium, Tokyo, Japan, 2011, pp. 214–215.
[34] S.L. Manzello, S. Suzuki, Y. Hayashi, NIST Special Publication 1126 (2011).
[35] S.L. Manzello, S. Suzuki, Y. Hayashi, Fire Saf. J. 54 (2012) 181–196.
[36] H. Yoshioka, H. Sato, Y. Omiya, Y. Hayashi, T. Noguchi, in: Proceedings of Annual Conference of the AIJ (Architectural Institute of Japan), Hokkaido, Japan, 2004, pp. 369–370. (in Japanese).
[37] D. Drysdale, An introduction to Fire Dynamics, third ed., John Wiley & Sons, Ltd., West Sussex, UK, 2011.
[38] K. Kishitani, S. Sugawara, H. Sato, Saigai no Kenkyu 13 (1982) 194–208.
[39] S.W. Lee, R.A. Davidson, J. Earthquake Eng. 14 (2010) 670–687.
[40] W. Mell, M.A. Jenkins, J. Gould, P. Cheney, Int. J. Wildland Fire 16 (2007) 1–22.